ISSN 1738-6055 (Print)
ISSN 2233-7660 (Online)

Lab Anim Res 2018: 34(4), 302-310
https://doi.org/10.5625/lar.2018.34.4.302

Laboratory Animal Research
http://submission.kalas.or.kr

CRISPR/Cas9-mediated knockout of *CD47* causes hemolytic anemia with splenomegaly in C57BL/6 mice

Joo-Il Kim[1,2,#], Jin-Sung Park[2,#], Jina Kwak[2], Hyun-Jin Lim[1,2], Soo-Kyung Ryu[2], Euna Kwon[2], Kang-Min Han[1,3], Ki-Taek Nam[4], Han-Woong Lee[5], Byeong-Cheol Kang[1,2,6,7,*]

[1]*Graduate School of Translational Medicine, Seoul National University College of Medicine, Seoul, Korea*
[2]*Department of Experimental Animal Research, Biomedical Research Institute, Seoul National University Hospital, Seoul, Korea*
[3]*Department of Pathology, Dongguk University Ilsan Hospital, Goyang, Korea*
[4]*College of Medicine Severance Biomedical Science Institute, Yonsei University, Seoul, Korea*
[5]*Department of Biochemistry, Yonsei University, Seoul, Korea*
[6]*Biomedical Center for Animal Resource and Development, Seoul National University, College of Medicine, Seoul, Korea*
[7]*Designed Animal and Transplantation Research Institute, Institute of Green Bio Science Technology, Seoul National University, Pyeongchang-gun, Korea*

CD47 (integrin-associated protein), a multi-spanning transmembrane protein expressed in all cells including red blood cells (RBCs) and leukocytes, interacts with signal regulatory protein α (SIRPα) on macrophages and thereby inhibits phagocytosis of RBCs. Recently, we generated a novel C57BL/6J *CD47* knockout (*CD47*$^{-/-}$ hereafter) mouse line by employing a CRISPR/Cas9 system at Center for Mouse Models of Human Disease, and here report their hematological phenotypes. On monitoring their birth and development, *CD47*$^{-/-}$ mice were born viable with a natural male-to-female sex ratio and normally developed from birth through puberty to adulthood without noticeable changes in growth, food/water intake compared to their age and sex-matched wild-type littermates up to 26 weeks. Hematological analysis revealed a mild but significant reduction of RBC counts and hemoglobin in 16 week-old male *CD47*$^{-/-}$ mice which were aggravated at the age of 26 weeks with increased reticulocyte counts and mean corpuscular volume (MCV), suggesting hemolytic anemia. Interestingly, anemia in female *CD47*$^{-/-}$ mice became evident at 26 weeks, but splenomegaly was identified in both genders of *CD47*$^{-/-}$ mice from the age of 16 weeks, consistent with development of hemolytic anemia. Additionally, helper and cytotoxic T cell populations were considerably reduced in the spleen, but not in thymus, of *CD47*$^{-/-}$ mice, suggesting a crucial role of CD47 in proliferation of T cells. Collectively, these findings indicate that our *CD47*$^{-/-}$ mice have progressive hemolytic anemia and splenic depletion of mature T cell populations and therefore may be useful as an *in vivo* model to study the function of CD47.

Keywords: CRISPR/Cas9, CD47, hemolytic anemia, splenomegaly

Received 27 November 2018; Revised version received 13 December; Accepted 14 December 2018

Immune system recognizes self and non-self using surface markers. CD47, also known as Integrin-Associated Protein (IAP), is a glycoprotein which ubiquitously exists on the surface of various cells including red blood cells (RBCs). CD47 functions as a "marker of self" on RBCs which prevents macrophages from phagocytosing self RBCs [1-4]. Also, it is a potential immunoregulatory molecule in integrin signaling as demonstrated in downregulation of T cell activation and IL-12 production by inactivating CD47 using thrombospondin-1 (TSP-1) or anti-CD47 monoclonal antibodies [5-8]. In addition, loss of CD47 in mice impaired resistance to *E. coli*

[#]These authors contributed equally to this work

*Corresponding author: Byeong-Cheol Kang, Graduate School of Translational Medicine, Seoul National University College of Medicine, 101 Daehakro, Jongno-gu, Seoul 03080, Korea
Tel: +82-2-2072-0841 ; Fax: +82-2-741-7620 ; E-mail: bckang@snu.ac.kr

injection by causing delay of polymorphonuclear leukocyte migration to the site of infection, indicating its role in cell migration [3]. Due to its role in immune response, *CD47* has been frequently knocked out with other immunity related genes such as *Recombination Activating Gene-2* (*Rag-2)* and γ*c* to create immune deficient animal models for transplantation studies [9, 10].

Generally, senescent RBCs are destroyed by splenic macrophages when they reach approximately 40-day-old [11]. However, destruction of RBCs in an early stage may occur in several conditions such as autoimmune disorders, genetic defects, drugs and red blood cell membrane instability, resulting in anemia. There are several types of anemia such as iron deficiency anemia, thalassemia, aplastic anemia, hemolytic anemia, sickle cell anemia and pernicious anemia. Among these, lack of CD47 expression in non-obese diabetic (NOD) mice has been associated with severe autoimmune hemolytic anemia, suggesting a crucial role of CD47 in maintaining the physiological levels of RBCs [12].

In this study, we report a novel *CD47* knockout (KO) mouse model (C57BL/6J-C*D47*^{em1hwl}/Korl, *CD47*$^{-/-}$ mice hereafter) that we generated using a CRISPR/Cas9 system at Center for Mouse Models of Human Disease (CMHD), and their hematological phenotypes. We found hemolytic anemia in 16-week-old *CD47*$^{-/-}$ mice, which was aggravated in 26 weeks. In addition, our *CD47*$^{-/-}$ mice had a defective immune system due to reduction of mature T cell populations in the spleen. These findings confirm the role of CD47 in blood cells, indicating that our *CD47*$^{-/-}$ mice may serve as a reliable platform to study the function of CD47.

Materials and Methods

Generation of *CD47*$^{-/-}$ mice and measurement of major physiological parameters

CD47$^{-/-}$ mice were generated in the C57BL/6J background using a CRISPR/Cas9 system as previously described [13]. For this study, heterozygous breeding pairs were used to produce *CD47*$^{-/-}$ mice and their wildtype (WT) littermates (n=7-9 per group). Ear tissues were used for genotyping in a conventional PCR with specific primers; forward; 5'-GGT CGG TCG TTT CCC TTG AA-3' and reverse; 5'-GAT CCC CGA GCC ACT CAC-3'. Mice were housed in an AAALAC International accredited specific pathogen free (SPF) facility (#001169) at Seoul National University Hospital under standard housing conditions 12 h dark/light cycle, 40-60% relative humidity and 22±2ºC with free access to food (LabDiet 5002 Certified Rodent Diet, PMI Nutrition International, USA) and water. All experiments were approved by the Institutional Animal Care and Use Committee in Seoul National University Hospital and animals were maintained in accordance with the Guide for the Care and Use of Laboratory Animals [14].

From 4 weeks after birth to 26 weeks, body weight and food/water intake of mice were measured once a week with daily observation of clinical signs. Measurement of food and water intake was carried out in the day cycle and calculated as the amount consumed per mouse during 24 hours.

Hematology, serum biochemistry and urinalysis

Hematology, serum biochemistry and urinalysis were carried out as described [15]. Briefly, at the age of 16 and 26 weeks, all mice were deeply anesthetized with isoflurane and peripheral blood was collected from the abdominal vein in a K_2EDTA contained tube (BD Microtainer, USA) for hematologic analysis using an ADVIA 2021i (Siemens Healthcare, USA). Serum biochemistry and urinalysis were carried out using a Hitachi 7070 (Hitachi, Tokyo, Japan) and a CLINTEK Adventus analyzer (Siemens Healthcare), respectively.

Histopathology

At necropsy, gross examination was performed for all organs. Then, major organs, except for eyes, testis and epididymis which were fixed in Davidson solution and Bouin's solution, respectively, were fixed in 10% neutral buffered formalin and embedded in paraffin wax after dehydration and clearing process. After sectioning in a thickness of 4-6 μm, tissues were stained with hematoxylin and eosin. To examine the levels of intracellular accumulation of iron in the spleens, we stained the tissue using Prussian blue reaction. Breifly, the paraffin-embedded spleen was sectioned and re-hydrated after deparaffinization. The tissue section was stained in freshly prepared 5% potassium ferrocyanide (Sigma Aldrich) in 10% HCl for 20 min and then counterstained with neutral red (Sigma Aldrich) for 5 minutes. All stained tissues were observed under a microscope (BX61, Olympus).

Flow cytometry

Cells were isolated from the spleens, bone marrow and thymuses of 16-week-age WT and *CD47*$^{-/-}$ mice (male; n=3 and female; n=3 per genotype) and stained with antibodies for flow cytometric analysis as described [15]. In this study, we used V450-anti-CD3e (500A2), FITC-anti-CD4 (RM4-5), APC-anti-CD5 (53-7.3), BV605-anti-CD8a (53-6.7), Alexa700-anti-CD19 (1D3), and PerCP-anti-CD45R (RA3-6B2) to label distinct lymphocyte populations. All antibodies employed in this study were from BD Bioscience and used at 1:200 except anti-CD4 antibody (1:500). After staining and washing, 20,000 cells were analyzed using a FACS Calibur (BD).

Statistics

All data were expressed as mean±SD, and statistical analysis was performed using a two-tailed *t* test in a SPSS software (version 22.0). $P<0.05$ was considered to be statistically significant.

Results and Discussion

Normal development of *CD47*$^{-/-}$ mice

To evaluate the role of CD47, we generated a novel *CD47*$^{-/-}$ mouse line by introducing a double-strand DNA break of CD47 exon 1 using a CRISPR/Cas9 system and inducing non-homologous end joining repair, which resulted in a deletion of 26 base pairs which created a frameshift mutation and a premature stop codon (Figure 1A).

To characterize the phenotype of *CD47*$^{-/-}$ mice, we first examined their development with monitoring of main physiological parameters including sex ratio, genotype, body weight gain, food and water intake for 26 weeks. At birth, there were no changes in the sex ratio of littermates (male; n=45, female; n=43 out of 88 siblings; *CD47*$^{-/-}$ male; n=13, *CD47*$^{-/-}$ female; n=12 out of 25 *CD47*$^{-/-}$mice), and the ratio of genotypes of mice born from *CD47*$^{+/-}$ parents was 1:1.6:0.8 for WT, *CD47*$^{+/-}$ and *CD47*$^{-/-}$, indicating a Mendelian inheritance

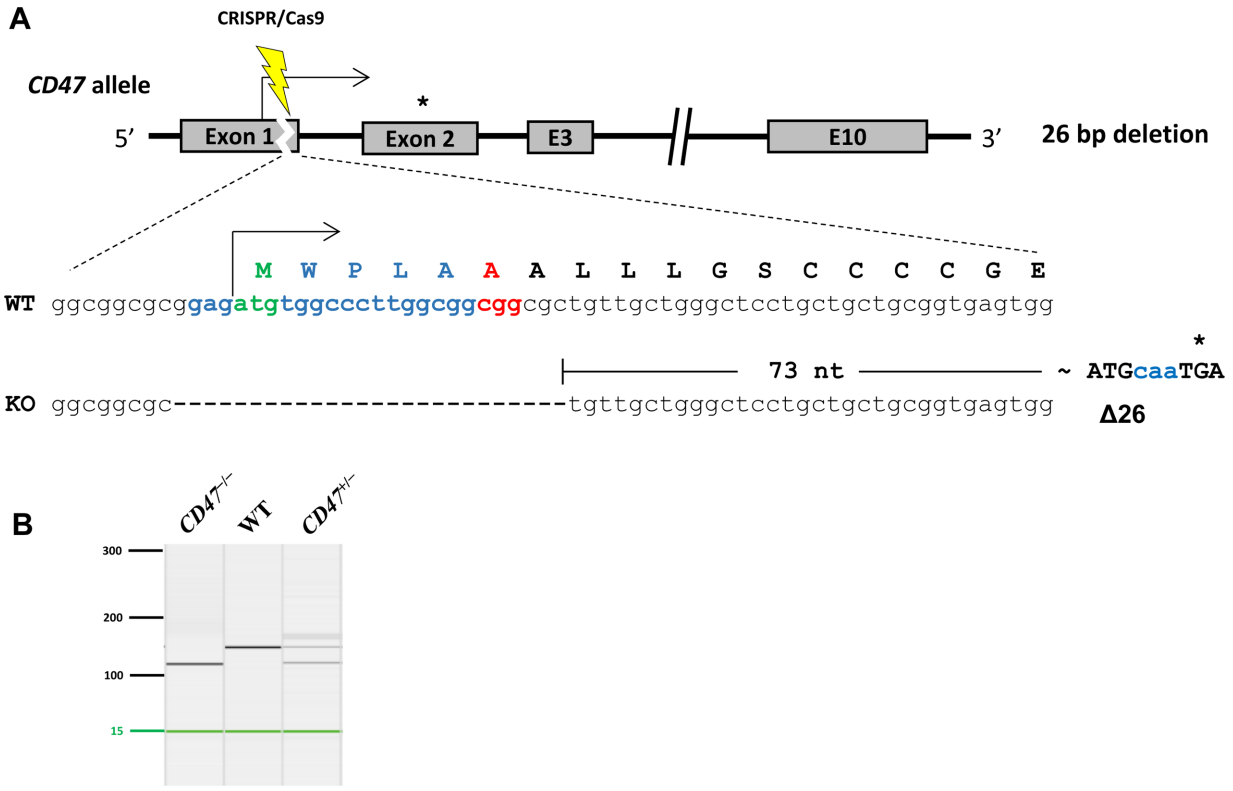

Figure 1. CRISPR/Cas9-mediated gene-targeting strategy to generate *CD47*$^{-/-}$ mice. (A) A schematic drawing shows the sequence of the *CD47* alleles in the wild-type (WT) and *CD47*$^{-/-}$ (KO) location of the start codon (green), RNA-guided engineered nucleases (RGEN) target sequence (blue) and protospacer adjacent motif (PAM; red). The double-strand break induced by the CRISPR/Cas9 was repaired by non-homologous end joining, resulting in a frameshift mutation by deleting 26 nucleotides and thereby creation of a premature termination codon (asterisk mark). (B) PCR products amplified from the targeted region of genomic DNA revealed genotypes of mice.

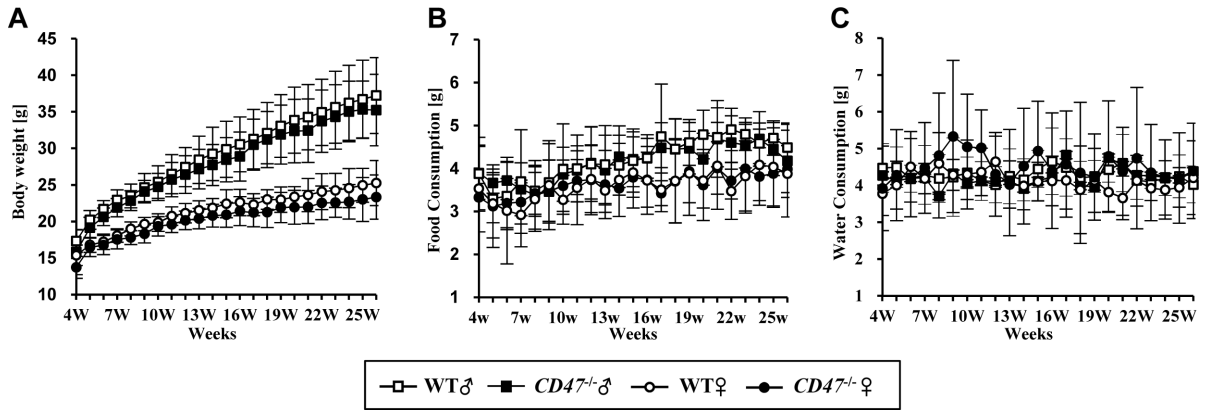

Figure 2. Body weight change, food and water consumption of *CD47*$^{-/-}$ mice. (A) The body weight, (B) daily food intake and (C) water consumption of wildtype (WT) and *CD47*$^{-/-}$ mice were measured weekly for 26 weeks. No significant change was observed in any of the parameters between WT male (open squares) and *CD47*$^{-/-}$ male (filled squares), and between WT female (open circles) and *CD47*$^{-/-}$ female (filled circles) mice.

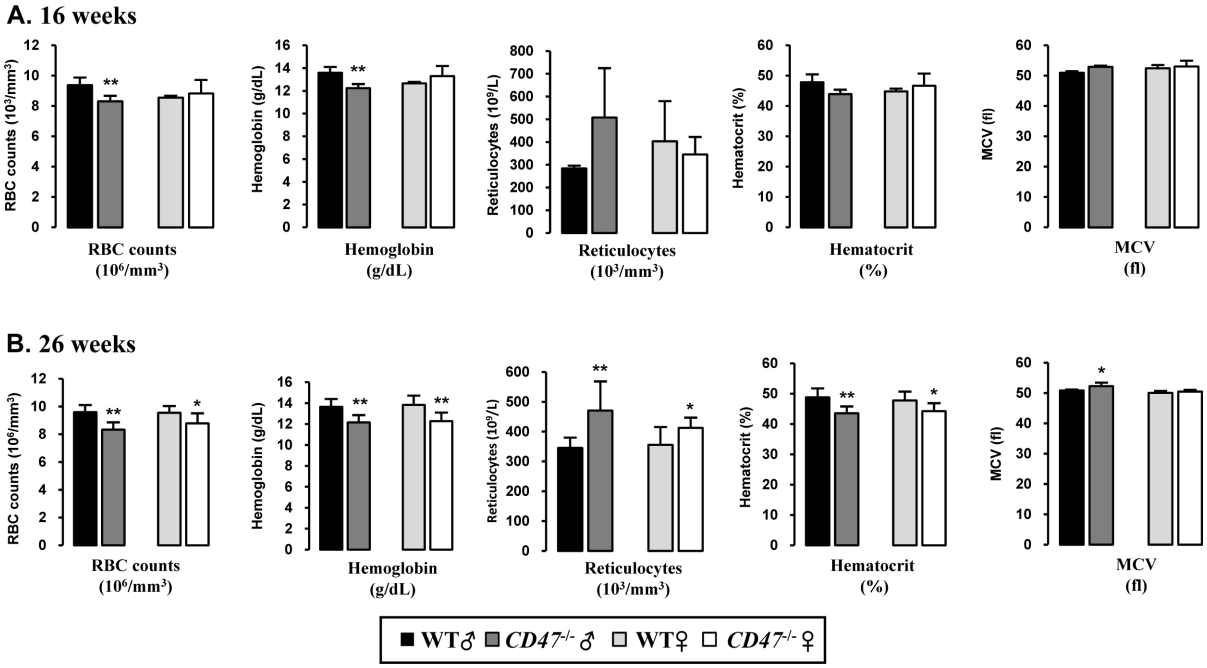

Figure 3. Hematological analysis of peripheral blood from *CD47*$^{-/-}$ mice. (A) 16 week-old of WT and *CD47*$^{-/-}$ mice (n=3 per group). Significant decrease of RBC counts and hemoglobin was observed in *CD47*$^{-/-}$ males compared to their wild-type counterparts (black bars for WT and dark gray bars for *CD47*$^{-/-}$ mice). (B) In the blood from 26 week-old of WT and *CD47*$^{-/-}$ mice (n=7 per group), RBC counts, hemoglobin and hematocrit were significantly declined in both male and female (light gray bars for WT and white bars for *CD47*$^{-/-}$ mice), while reticulocyte counts in both genders and mean corpuscular mean volume (MCV) only in male were increased. **P*<0.05 and ***P*<0.01.

pattern of the knockout alleles with no embryonic lethality. For 26 weeks, body weight gain and food/water consumption of *CD47*$^{-/-}$ mice was comparable to WT (Figure 2), suggesting that loss of the *CD47* gene did not affect the postnatal development.

Progressive anemia in *CD47*$^{-/-}$ mice

When peripheral blood was collected from 16-week-old mice and analyzed, male CD47$^{-/-}$ mice showed a significant reduction of RBC counts (11.4 %, $P<0.01$) and hemoglobin (10.1%, $P<0.01$) at the age of 16 weeks, while no abnormality was observed in the blood of female CD47$^{-/-}$ mice (Figure 3A). The anemia-like feature observed in male CD47$^{-/-}$ mice became more evident at 26weeks with increase of reticulocytes (136.2%, $P<0.01$) and MCV (102.5%, $P<0.05$) in

Table 1. Serum biochemistry of *CD47*$^{-/-}$ mice

Parameters		WT male (n=7)	*CD47*$^{-/-}$ male (n=7)	WT female (n=9)	*CD47*$^{-/-}$ female (n=8)
BUN	(mg/dL)	23.3±9.5	22.9±3.4	18.6±2.9	22.8±4.9
Chol	(mg/dL)	112.7±23.4	119.9±8.4	86.1±16.8	81.9±15.0
T.protein	(g/dL)	4.5±0.4	4.4±0.4	4.5±0.3	4.6±0.3
Albumin	(g/dL)	1.6±0.1	1.7±0.1	1.7±0.1	1.7±0.1
T.bil	(mg/dL)	0.05±0.02	0.06±0.04	0.08±0.04	0.04±0.04
ALP	(IU/L)	194.2±48.1	211.4±32.6	288.3±70.4	310.3±53.3
AST	(IU/L)	83.7±64.1	111.7±104.5	110.1±95.0	113.5±34.6
ALT	(IU/L)	32.8±15.7	42.1±31.6	51.1±58.2	44.6±16.1
γGT	(IU/L)	-0.5±1.2	-0.6±0.8	0.2±0.7	-0.3±0.9
Creatinine	(mg/dL)	0.28±0.03	0.29±0.06	0.25±0.12	0.28±0.10
TG	(mg/dL)	52.0±25.3	51.7±24.5	23.6±6.4	37.6±25.9
Glu	(mg/dL)	251.0±43.5	262.4±17.9	275.8±38.3	264.6±38.9

*__Abbreviation.__ Blood urea nitrogen (BUN), cholesterol (Chol), total protein (T.protein), total bilirubin (T.bil), alkaline phosphatase (ALP), aspartate aminotransferase (AST), alanine aminotransferase (ALT), gamma (γ)-glutamyl transferase (γGT), triglyceride (TG), glucose (Glu).

addition to the reduction of RBC counts (13.1%, P<0.01), hemoglobin (10.9%, P<0.01) and hematocrit (10.7%, P<0.01) as shown in Figure 3B. 26-week-old female *CD47*$^{-/-}$ mice also showed similar changes in the parameters for erythrocytes; reduction of RBC counts (8.0%, P<0.05), hemoglobin (11.1%, P<0.01) and hematocrit (7.5%, P<0.05) with increased reticulocytes (116.0%, P<0.05). These findings indicate the development of anemia in our *CD47*$^{-/-}$ mice, which is progressively aggravated over aging.

Serum biochemistry (Table 1) and urinalysis (data not shown) showed no changes between *CD47*$^{-/-}$ mice and their WT littermates, suggesting that lack of *CD47* may not affect the function of other organs, especially liver and kidney.

Splenomegaly with intracellular iron accumulation in *CD47*$^{-/-}$ mice

Based on the function of CD47 in RBCs, anemia observed in our *CD47*$^{-/-}$ mice was possibly caused by

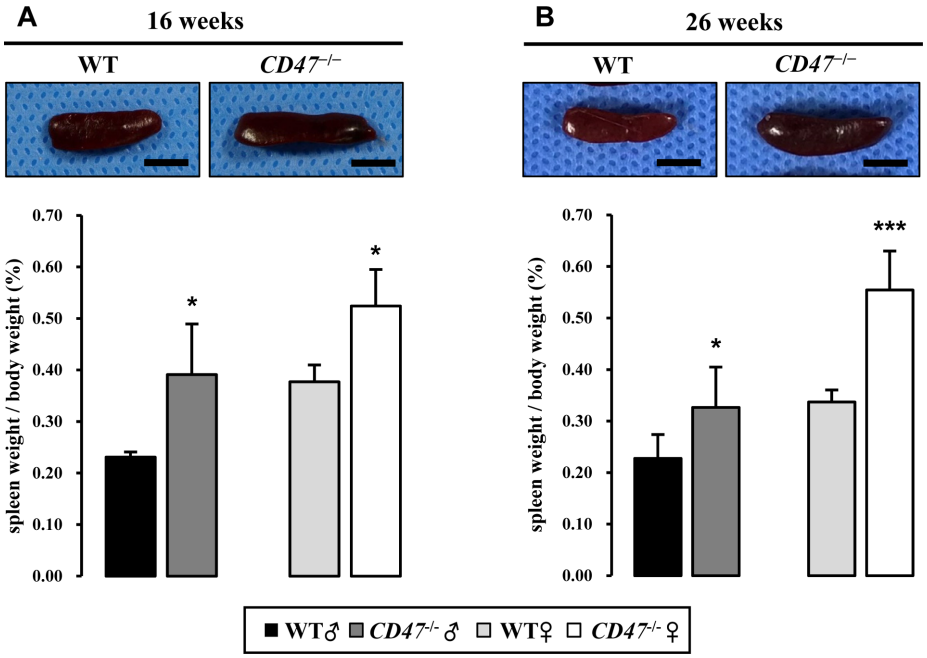

Figure 4. Increased size and weight of spleens in *CD47*$^{-/-}$ mice. Representative images and bar graphs show increased size and weight of spleens in the 16 week-old (A) and 26 week-old (B) *CD47*$^{-/-}$ mice compared to their respective wild-type littermates. The graphs are expressed as a percentage of organ weight/body weight (black bars, WT male; dark gray bars, *CD47*$^{-/-}$ male; light gray bars, WT female; and white bars, *CD47*$^{-/-}$ female mice). Scale bar; 5 mm. *P<0.05 and ***P<0.001.

Table 2. Absolute and relative weight of major organs of 26-week-old *CD47*$^{-/-}$ mice

Organ		WT male (n=7)	*CD47*$^{-/-}$ male (n=7)	WT female (n=9)	*CD47*$^{-/-}$ female (n=8)
Body weight	(g)	38.03±4.56	35.03±3.94	24.67±3.11	23.29±2.75
Liver	(g)	1.71±0.25	1.69±0.28	1.04±0.18	1.04±0.14
	(g%)	4.53±0.62	4.79±0.31	4.19±0.24	4.46±0.29
Spleen	(g)	0.09±0.01	**0.11±0.02***	0.08±0.01	**0.13±0.02*****
	(g%)	0.23±0.05	**0.33±0.08***	0.34±0.02	**0.55±0.08*****
Kidney (right)	(g)	0.20±0.03	0.18±0.03	0.13±0.01	0.12±0.01
	(g%)	0.53±0.08	0.52±0.06	0.54±0.05	0.52±0.05
Kidney (left)	(g)	0.20±0.03	0.18±0.02	0.13±0.02	0.12±0.01
	(g%)	0.54±0.12	0.52±0.05	0.52±0.04	0.51±0.05
Adrenal gland	(g)	0.0013±0.0006	0.0014±0.0040	0.0032±0.0009	0.0027±0.0006
(right)	(g%)	0.0033±0.0014	0.0040±0.0014	0.0130±0.0027	0.0117±0.0022
Adrenal gland	(g)	0.0012±0.0004	0.0015±0.0005	0.0033±0.0008	0.0035±0.0010
(left)	(g%)	0.0031±0.0010	0.0045±0.0017	0.0132±0.0029	0.0151±0.0039
Testis (right)	(g)	0.12±0.02	0.11±0.01	0.0045±0.0008	0.0030±0.0010
/ovary (right)	(g%)	0.32±0.05	0.32±0.03	0.0187±0.0047	0.0132±0.0044
Testis (left)	(g)	0.11±0.01	0.11±0.01	0.0037±0.0012	0.0028±0.0009
/ovary (left)	(g%)	0.30±0.05	0.32±0.02	0.0150±0.0048	0.0122±0.0041
Thymus	(g)	0.05±0.01	0.04±0.01	0.05±0.01	0.04±0.01
	(g%)	0.13±0.01	0.11±0.01	0.19±0.02	0.19±0.03
Heart	(g)	0.15±0.02	0.15±0.02	0.12±0.01	0.12±0.02
	(g%)	0.40±0.05	0.44±0.06	0.50±0.04	0.50±0.07
Lung	(g)	0.15±0.01	0.15±0.01	0.14±0.01	0.14±0.01
	(g%)	0.40±0.06	0.43±0.06	0.58±0.06	0.60±0.10
Brain	(g)	0.46±0.03	0.46±0.02	0.47±0.01	0.48±0.01
	(g%)	1.23±0.16	1.33±0.13	1.93±0.23	2.08±0.25

*P<0.05 and ***P<0.001 in comparison to respective gender-matching WT mice

increased hemolysis. As spleen is commonly enlarged in hemolytic anemia due to accumulation of RBCs and macrophages [16,17], we examined the organs of *CD47*$^{-/-}$ mice with a particular focus on their spleens. While no changes were found in other organs of CD47$^{-/-}$ mice, spleens of *CD47*$^{-/-}$ mice were found to be significantly larger than those of WT littermates (Figure 4, Table 2). When the organ per body weight ratio was calculated, both genders of 16-week-old *CD47*$^{-/-}$ mice exhibited enlarged spleens (Figure 4A; 169.3% increase compared to WT male, 139.0 % for female mice, P<0.05 for both). In line with the progression of anemia observed in hematological analysis, splenomegaly was consistently observed in both genders of 26 week-old *CD47*$^{-/-}$ mice (Figure 4B; 143.5 % increase in male, P<0.05 and 161.8 % in female, P<0.001). Except for the spleen, no other organs in *CD47*$^{-/-}$ mice showed notable changes (Table 2).

When the spleen was histopathologically examined, cells containing brown-gold pigments were more frequently observed in *CD47*$^{-/-}$ mice compared to WT mice (Figures 5A, 5B). As loss of CD47 was previously associated with increased destruction of RBCs by macrophages, these pigments were likely hemosiderins derived from increased degradation of iron-containing hemoglobins in RBCs and therefore we visualized intracellular iron in the tissue using Prussian blue reaction to determine the identity of the pigments. Staining of iron revealed noticeable increase in the number of dark blue-stained cells with a tendency of higher intracellular staining levels in *CD47*$^{-/-}$ mice than WT mice (Figures 5C, 5D), indicating the increased intracellular accumulation of hemosiderns. It is tempting to postulate that these hemosiderin-containing cells were macrophages due to their function in hemolysis, but this proposition may need to be confirmed. There are several types of anemia reported in humans. Among them, the anemia identified in our *CD47*$^{-/-}$ mice is likely hemolytic based on the following observations; *CD47*$^{-/-}$ mice showed concurrent reduction of RBC counts, hemoglobins and hematocrit with increased reticulocytes, indicating loss of mature RBCs with increased release of immature RBCs into the blood as a compensatory response. Although the anemic feature was not evident in 16-

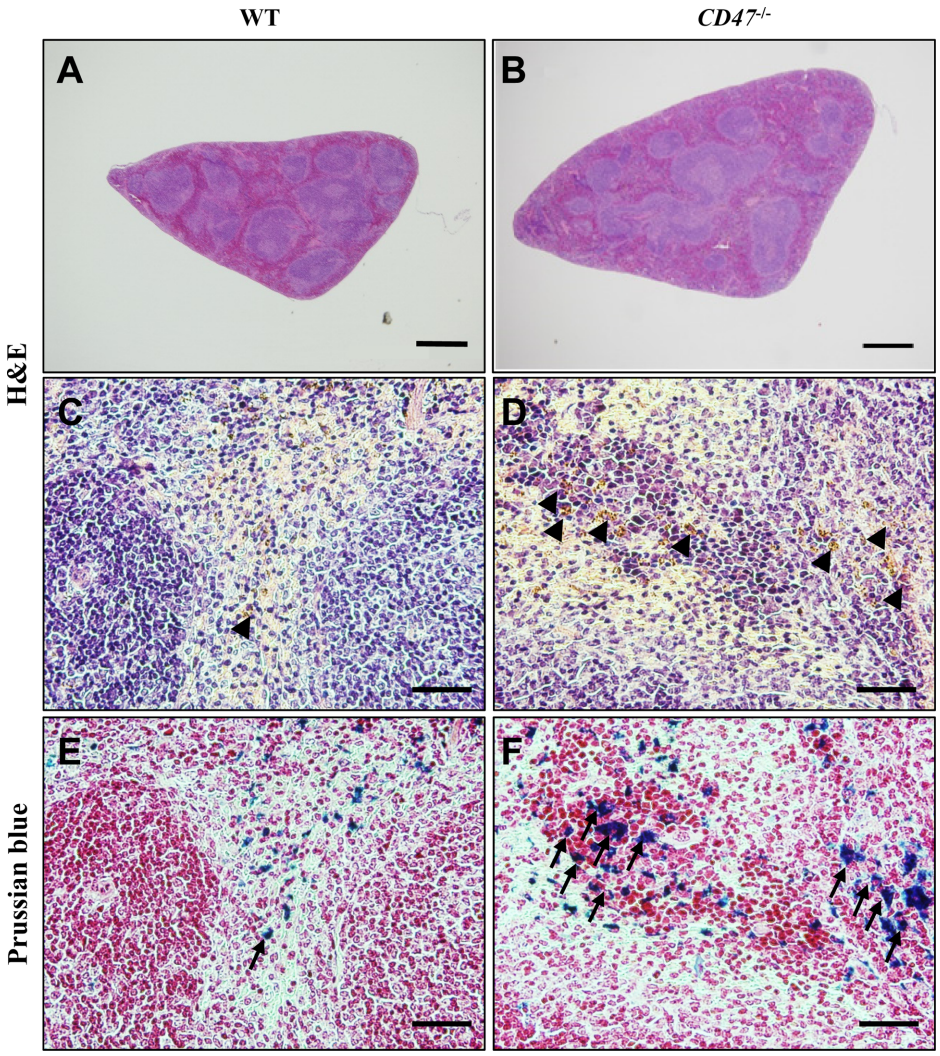

Figure 5. Intracellular accumulation of iron-containing hemosiderin in the splenic cells of 26-week-old *CD47*$^{-/-}$ mice. Representative images of H&E stained spleen tissues from WT (A and C) and *CD47*$^{-/-}$ mice (B and D) show brown-gold pigmented cells (arrowheads). The pigmented cells were more frequently observed in *CD47*$^{-/-}$ compared to WT mice. Prussian blue staining (E and F) revealed that there were more iron-accumulated cells (arrows) in the spleens of *CD47*$^{-/-}$ mice than WT. Scale bars for the images with low magnification (x10) and high magnification (x60) are 250 and 2 μm, respectively.

week-old female mice, both genders of *CD47*$^{-/-}$ mice had enlargement of the spleen which continued to the age of 26 weeks with concurrent aggravation of hematological parameters regarding RBCs. Furthermore, the elevated destruction of RBCs was demonstrated by the increased number of hemosiderin-loaded cells with higher amount of hemosiderins accumulated in each cells of the *CD47*$^{-/-}$ spleens, strongly supporting our hypothesis. Despite these findings, our data however do not exclude the possibility of other types of anemia with similar features. Therefore, further investigation is warranted to characterize the type and clinical manifestation of the anemia in our *CD47*$^{-/-}$ mice.

The findings on the development of hemolytic anemia in our *CD47*$^{-/-}$ mice have not been reported in the previously generated *CD47*$^{-/-}$ mice [4], but were closely in line with AIHA in *CD47*$^{-/-}$ NOD mice [12] with several different features noted; *CD47*$^{-/-}$ NOD mice showed much greater reduction of hematocrit than our *CD47*$^{-/-}$ mice, while jaundice was only observed in *CD47*$^{-/-}$ NOD mice, suggesting a mild degree of hemolytic anemia in our mice. The mouse strains used in generating models (NOD vs. C57Bl/6) may have played a role in causing these discrepancies in manifestation of hemolytic anemia between the two mouse lines.

Reduction of T cells in the spleen of *CD47*$^{-/-}$ mice

Next, we examined changes in subpopulations of

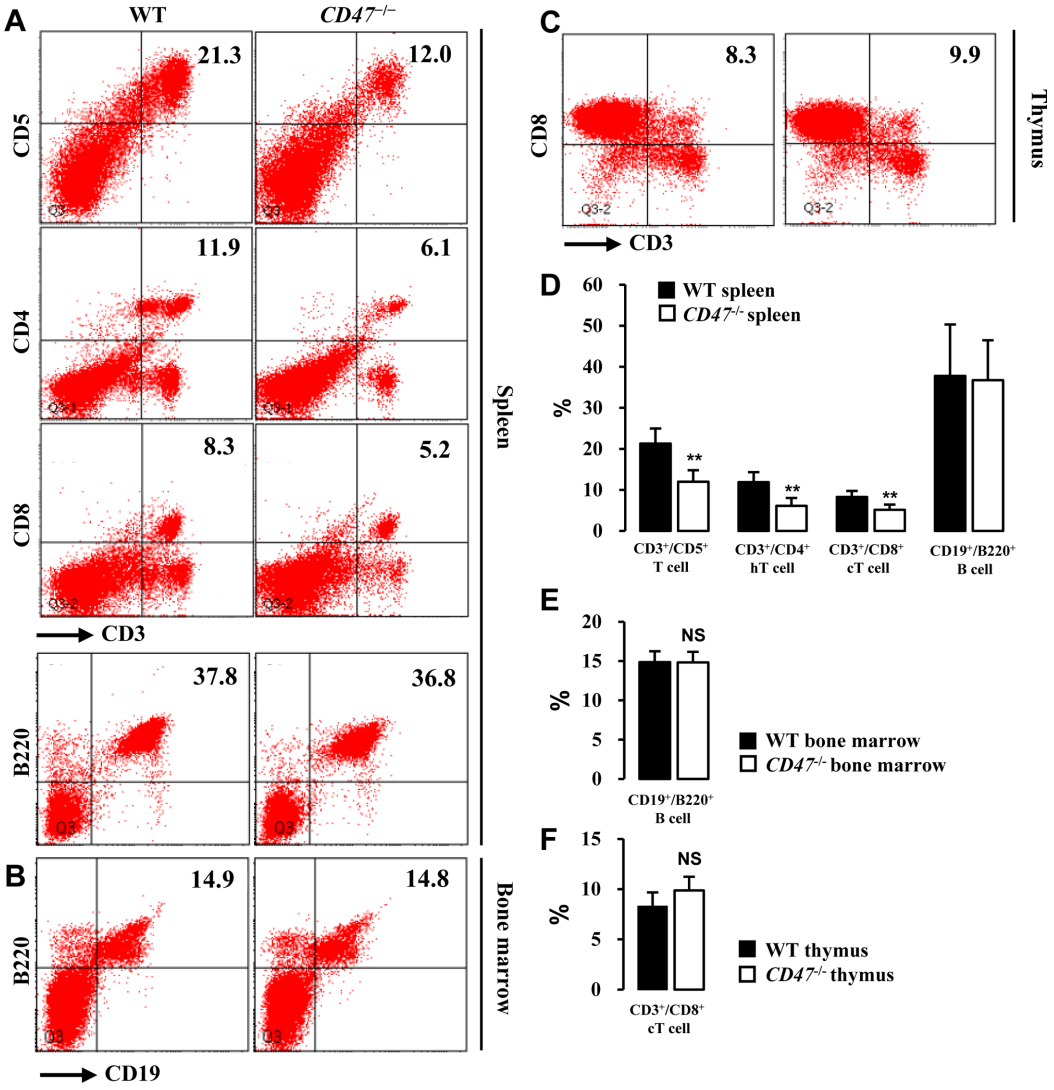

Figure 6. Flow cytometric analysis of cells isolated from the spleens, thymuses and bone marrow of *CD47*$^{-/-}$ mice. (A and D) Dot plots display CD3$^+$CD5$^+$, CD3$^+$CD4$^+$ and CD3$^+$CD8$^+$ T cell populations as well as CD19$^+$B220$^+$ B cell population in the spleen. All the T cell populations detected here were significantly decreased in *CD47*$^{-/-}$ mice compared to WT. (B and E) Cells from the bone marrow show no changes in CD19$^+$B220$^+$ B cells between WT and *CD47*$^{-/-}$ mice. (C and F) The numbers of CD3$^+$CD8$^+$ T cells isolated from thymuses are comparable between WT and *CD47*$^{-/-}$ mice. ***P*<0.01, NS: Not significant.

lymphocytes including T and B cells in *CD47*$^{-/-}$ mice as inactivation of CD47 previously resulted in reduction of T cell populations in the spleen [18]. To assess the impact of CD47 deficiency on those lymphocytes, we performed flow cytometry on the cells isolated from 16-week-old mice spleens, thymuses and bone marrow. Flow cytometry analysis on splenic lymphocytes revealed a remarkable reduction of CD3$^+$CD5$^+$, CD3$^+$CD4$^+$ and CD3$^+$CD8$^+$ T cells (Figures 6A, 6C, P<0.01 for all), while no change was found in CD19$^+$B220$^+$ B cell population. The number of CD19$^+$B220$^+$ B cells from the bone marrow of *CD47*$^{-/-}$ mice was also comparable to WT (Figures 6B, 6D). Our findings recapitulated the crucial role of CD47-SIRPα interaction on T cell proliferation as similar findings on the reduction of CD4$^+$ T cells have been reported in the spleen of the CD47 binding partner SIRPα-deficient mice [18]. Contrary to the reduction of T cells in the spleen, no change was detected in thymic T cell populations when compared to WT (Figures 6C, 6F), suggesting differential roles of CD47 in T cells depending on their developmental stage; CD47 functions in the proliferation of T cells which occurs in the spleen, but not at the stage of initial development through negative selection in the thymus [19].

In this study, we generated a novel *CD47*$^{-/-}$ C57BL/6J

mouse line using a CRISPR/Cas9 system and found a progressive hemolytic anemia as well as profound reduction of mature T cell populations in the spleen. Intriguingly, despite its ubiquitous expression, loss of CD47 mainly resulted in hematological phenotypes without causing embryonic lethality, developmental defects or any noticeable changes in the structure and function of other tissues, indicating its preferred function in blood cells. These results, however, do not exclude the possible role of CD47 in other types of cells and further investigation may be required to reveal cell-specific impact of CD47 deficiency. In conclusion, CRISPR/Cas9-mediated generation of *CD47*$^{-/-}$ mice confirmed the function of CD47 in the maintenance of RBC and T cell populations, demonstrating their usefulness as an *in vivo* platform to study the function of CD47.

Acknowledgment

This research was supported by a grant (14182 MFDS978) from Ministry of Food and Drug Safety in 2017.

Conflict of interests The authors declare that there is no financial conflict of interests to publish these results.

References

1. Lindberg FP, Lublin DM, Telen MJ, Veile RA, Miller YE, Donis-Keller H, Brown EJ. Rh-related antigen CD47 is the signal-transducer integrin-associated protein. J Bio Chem 1994; 269(3): 1567-1570.
2. Reinhold MI, Lindberg FP, Plas D, Reynolds S, Peters MG, Brown EJ. In vivo expression of alternatively spliced forms of integrin-associated protein (CD47). J Cell Sci 1995; 108(11): 3419-3425.
3. Lindberg FP, Bullard DC, Caver TE, Gresham HD, Beaudet AL, Brown EJ. Decreased resistance to bacterial infection and granulocyte defects in IAP-deficient mice. Science 1996; 274(5288): 795-798.
4. Oldenborg PA, Zheleznyak A, Fang Y-F, Lagenaur CF, Gresham HD, Lindberg FP. Role of CD47 as a marker of self on red blood cells. Science 2000; 288(5473): 2051-2054.
5. Armant M, Avice M-N, Hermann P, Rubio M, Kiniwa M, Delespesse G, Sarfati M. CD47 ligation selectively downregulates human interleukin 12 production. J Exp Med 1999; 190(8): 1175-1182.
6. Demeure CE, Tanaka H, Mateo V, Rubio M, Delespesse G, Sarfati M. CD47 engagement inhibits cytokine production and maturation of human dendritic cells. J Immunol 2000; 164(4): 2193-2199.
7. Mateo V, Lagneaux L, Bron D, Biron G, Armant M, Delespesse G, Sarfati M. CD47 ligation induces caspase-independent cell death in chronic lymphocytic leukemia. Nat Med 1999; 5(11): 1277-1284.
8. Waclavicek M, Majdic O, Stulnig T, Berger M, Baumruker T, Knapp W, Pickl WF. T cell stimulation via CD47: agonistic and antagonistic effects of CD47 monoclonal antibody 1/1A4. J Immunol 1997; 159(11): 5345-5354.
9. Lavender KJ, Pang WW, Messer RJ, Duley AK, Race B, Phillips K, Scott D, Peterson KE, Chan CK, Dittmer U, Dudek T, Allen TM, Weissman IL, Hasenkrug KJ. BLT-humanized C57BL/6 Rag2-/-γc-/-CD47-/- mice are resistant to GVHD and develop B- and T-cell immunity to HIV infection. Blood 2013; 122(25): 4013-4020.
10. Lavender KJ, Messer RJ, Race B, Hasenkrug KJ. Production of bone marrow, liver, thymus (BLT) humanized mice on the C57BL/6 Rag2(-/-)γc(-/-)CD47(-/-) background. J Immunol Methods 2014; 407: 127-134.
11. VAN PUTTEN LM, Croon F. The life span of red cells in the rat and the mouse as determined by labeling with DFP32 in vivo. Blood 1958; 13(8): 789-794.
12. Oldenborg PA, Gresham HD, Chen Y, Izui S, Lindberg FP. Lethal autoimmune hemolytic anemia in CD47-deficient nonobese diabetic (NOD) mice. Blood 2002; 99(10): 3500-3504.
13. Lee JH, Park JH, Nam TW, Seo SM, Kim JY, Lee HK, Han JH, Park SY, Choi YK, Lee HW. Differences between immunodeficient mice generated by classical gene targeting and CRISPR/Cas9-mediated gene knockout. Transgen Res 2018; 27(3): 241-251.
14. Council NR. Guide for the care and use of laboratory animals: National Academies Press; 2010.
15. Kim JI, Park JS, Kim H, Ryu SK, Kwak J, Kwon E, Yun JW, Nam KT, Lee HW, Kang BC. CRISPR/Cas9-mediated knockout of Rag-2 causes systemic lymphopenia with hypoplastic lymphoid organs in FVB mice. Lab Anim Res 2018; 34(4): 166-175.
16. Wennberg E, Weiss L. Splenomegaly and hemolytic anemia induced in rats by methylcellulose-an electron microscopic study. J Morphol 1967; 122(1): 35-61.
17. Wagner KU, Claudio E, Rucker EB 3rd, Riedlinger G, Broussard C, Schwartzberg PL, Siebenlist U, Hennighausen L. Conditional deletion of the Bcl-x gene from erythroid cells results in hemolytic anemia and profound splenomegaly. Development 2000; 127(22): 4949-4958.
18. Sato-Hashimoto M, Saito Y, Ohnishi H, Iwamura H, Kanazawa Y, Kaneko T, Kusakari S, Kotani T, Mori M, Murata Y, Okazawa H, Ware CF, Oldenborg PA, Nojima Y, Matozaki T. Signal regulatory protein α regulates the homeostasis of T lymphocytes in the spleen. J Immunol 2011; 187(1): 291-297.
19. Guimont-Desrochers F, Beauchamp C, Chabot-Roy G, Dugas V, Hillhouse EE, Dusseault J, Langlois G, Gautier-Ethier P, Darwiche J, Sarfati M, Lesage S. Absence of CD47 in vivo influences thymic dendritic cell subset proportions but not negative selection of thymocytes. Int Immunol 2009; 21(2): 167-177.